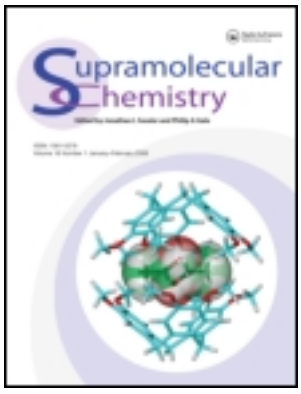

Supramolecular Chemistry
Publication details, including instructions for authors and subscription information:
http://www.tandfonline.com/loi/gsch20

Bigger, better, faster: molecular shuttles with sterically non-hindering biisoquinoline chelates

Fabien Durola [a], Jacques Lux [b], Jean-Pierre Sauvage [b] & Oliver S. Wenger [c]

[a] Centre de Recherche Paul Pascal, Pessac, France

[b] Université de Strasbourg, Strasbourg, France

[c] University of Goettingen, Goettingen, Germany

Available online: 31 Aug 2010

To cite this article: Fabien Durola, Jacques Lux, Jean-Pierre Sauvage & Oliver S. Wenger (2011): Bigger, better, faster: molecular shuttles with sterically non-hindering biisoquinoline chelates, Supramolecular Chemistry, 23:01-02, 42-52

To link to this article: http://dx.doi.org/10.1080/10610278.2010.510189

Supramolecular Chemistry
Vol. 23, Nos. 1–2, January–February 2011, 42–52

Bigger, better, faster: molecular shuttles with sterically non-hindering biisoquinoline chelates

Fabien Durola[a], Jacques Lux[b], Jean-Pierre Sauvage[b]* and Oliver S. Wenger[c]

[a]*Centre de Recherche Paul Pascal, Pessac, France;* [b]*Université de Strasbourg, Strasbourg, France;* [c]*University of Goettingen, Goettingen, Germany*

(*Received 21 May 2010; final version received 15 July 2010*)

In the past, a variety of mechanically interlocked systems such as catenanes and rotaxanes were constructed on the basis of Cu(I) coordination chemistry and endocyclic 1,10-phenanthroline ligands. This review reports on the coordination chemistry of a new family of endocyclic bidentate chelators that are sterically non-hindering, namely 8,8′-diaryl-substituted 3,3′-biisoquinolines. These ligands allow the construction of new multi-component assemblies that are inaccessible with the previously investigated 1,10-phenanthrolines. On the one hand, the sterically non-hindering nature of the new endocyclic chelators makes three-component entanglements around octahedral metal centres such as iron(II), cobalt(II) and ruthenium(II) readily possible. On the other hand, it permits the construction of copper-based molecular shuttles that exhibit shuttling kinetics that excels over those of previously investigated analogous systems with 1,10-phenanthrolines. Thus, within this class of molecular machines, a bigger chelator leads to faster molecular movement, i.e. to a better performance of the molecular machine.

Keywords: molecular shuttles; copper; biisoquinoline; chelates

1. Introduction

The field of molecular machines is vast, and there is a large variety of different ways how mechanically interlocked molecules can be assembled and set into motion (*1–9*). One possibility, applied since many years in the Strasbourg group, involves the use of coordination chemistry (*10–15*). Indeed, transition metals are particularly well suited for gathering various organic building blocks and disposing them in a given spatial arrangement. Thanks to its well-defined tetrahedral coordination geometry, Cu(I) has been particularly useful for the construction of many catenanes and rotaxanes (*16–20*). A key ingredient on this route to multi-component assemblies are bidentate chelators that can be incorporated into a molecular ring in an endocyclic fashion. This is the case, for example, for 2,9-disubstituted 1,10-phenanthroline or 6,6′-disubstituted 2,2′-bipyridine. As seen from Scheme 1, the endocyclic coordination mode can only be enforced with these two particular substitution patterns. Any substitution other than in α-position to the nitrogen atoms will either lead to a mixture of endocyclic and exocyclic species or to preferred exocyclic coordination.

The 2,9-diphenyl-1,10-phenanthroline (dpp) fragment has played a particularly prominent role due to its extended rigid backbone. This chelator forms very stable $[Cu(dpp)_2]^+$ complexes with endocyclic coordination, and mechanically interlocked molecules can be obtained through macrocyclisation via flexible polyethylene glycol chains attached to the dpp-phenyls and subsequent removal of the metal (*21*, *22*). While this approach to obtaining catenanes and rotaxanes has been very successful, it also has its limitations. Firstly, steric constraints impede the formation of complexes in which three dpp fragments gather around a single octahedral metal centre: the dpp ligand is simply too small for this purpose. Secondly, molecular shuttles that involve the $[Cu(dpp)_2]^+$ fragment exhibit rather slow shuttling kinetics which also has to do with the fact that the dpp ligands are sterically demanding (*13*). They shield the copper centre too well from the solvent, and this decelerates ligand exchange reactions very significantly. Hence, the overall shuttling process, which presumably requires the exchange of one dpp ligand by solvent molecules, is becoming slow.

These two important drawbacks of the dpp ligands have provided the motivation for the search of a new family of bidentate chelators that could be included in macrocycles in an endocyclic but sterically non-hindering fashion. Our search has been successful with the synthesis of 8,8′-disubstituted 3,3′-biisoquinolines (*23*, *24*). Here, we review the coordination chemistry of these new ligands on a few selected examples (Section 2), and we report on molecular shuttles that are based on the coordination chemistry of these ligands (Section 3).

2. Coordination chemistry of 8,8′-disubstituted 3,3′-biisoquinolines

As seen from Scheme 2, there are certain analogies between the long-known dpp-ligands and the newly

*Corresponding author. Email: sauvage@chimie.u-strasbg.fr

ISSN 1061-0278 print/ISSN 1029-0478 online

DOI: 10.1080/10610278.2010.510189
http://www.informaworld.com

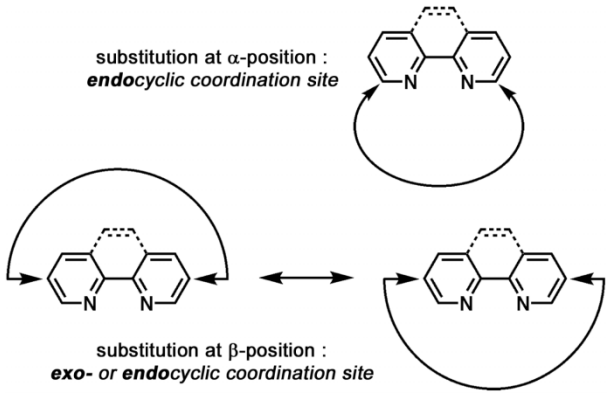

Scheme 1. 2,9-Substitution of 1,10-phenanthroline and 6,6′-substitution of 2,2′-bipyridine results in macrocycles with endocyclic coordination. Substitution at other positions is expected to lead to both *endo*- and *exo*-cyclic macrocycles.

synthesised 8,8′-disubstituted 3,3′-biisoquinolines, but there are also some very important differences. Although both types of ligands are bidentate chelators, the biisoquinolines have no substituents at the α-positions to the chelating nitrogen atoms, which is in contrast to the dpp molecules. Common to both ligands is the crescent shape, thereby allowing the incorporation of each of these ligands in a ring with an endocyclic coordination site, but the 8,8′-diphenyl-substituted 3,3′-biisoquinoline fragment (dpbiiq) offers a much more open coordination site than the dpp ligand: the distance between the phenyl rings attached to the 3,3′-biisoquinoline backbone is roughly 11 Å, whereas for the 1,10-phenanthroline backbone, it is only about 7 Å (*25*). Indeed, in the biisoquinoline ligand, the coordinated metal centre will be rather remote from the phenyl rings used to ensure the endocyclic coordination mode.

The synthesis of the 8,8′-disubstituted biisoquinolines proceeds over several synthetic steps, yet it is possible to produce gram-scale quantities of a variety of molecules of this type in a reasonable amount of time (*24*). We explored the synthesis of 3,3′-biisoquinolines that bear phenyl or biphenyl substituents at the 8 and 8′ positions, but encountered serious solubility problems with the latter. A key finding is that with these new ligands, it is possible to

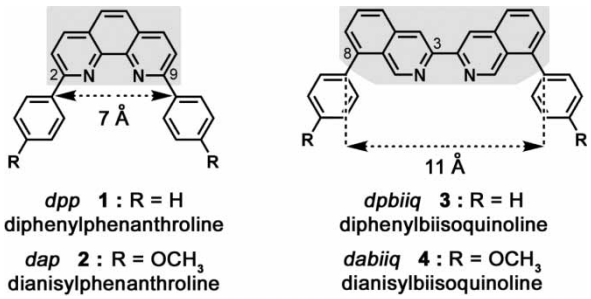

Scheme 2. Endocyclic ligands based on ddp and dpbiiq.

form homoleptic complexes in which three such ligands are coordinated to one single metal centre (*26*). This is illustrated by Figure 1 which shows the chemical formulas and X-ray crystal structures of a ruthenium(II) complex with three 8,8′-dianisyl-3,3′-biisoquinoline ligands (left) and an iron(II) complex with three 8,8′-diphenylanisyl-3,3′-biisoquinoline ligands (right).

The successful synthesis of the complexes from Figure 1 confirms the initial hypothesis formulated at the outset of this research. Clearly, the new biisoquinoline ligands are sterically non-hindering despite their endocyclic coordination modes. The three-component entanglements of three crescent-shaped chelates coordinated to a single octahedral metal centre result in more or less symmetrical helical pseudo-D_3 structures. The endotopic cleft distances, i.e. the distances between the oxygen atoms attached to two different anisyls on a given 3,3′-biisoquinoline, range from 15.6 to 16.4 Å in the case of the ruthenium complex with the shorter 8,8′-dianisyl-3,3′-biisoquinoline ligand, and from 18.7 to 20.9 Å in the iron(II) complex with the longer 8,8′-diphenylanisyl-3,3′-biisoquinoline ligand (*26*, *27*). These structures are not only aesthetically pleasing, but they also form the basis for multi-component assemblies with new chemical topologies, a branch of research that we have reviewed recently (*28*). Here, we intend to focus on the use of the sterically non-hindering ligand family for the construction of new copper-based molecular machines.

2.1 Fast-moving molecular shuttles based on copper coordination chemistry and biisoquinoline macrocycles

Molecular shuttles (*29–43*) constitute a subclass of molecular machines. Typically, they contain a molecular ring that can glide along an axis on which it has been threaded, whereby the motion can be triggered at will

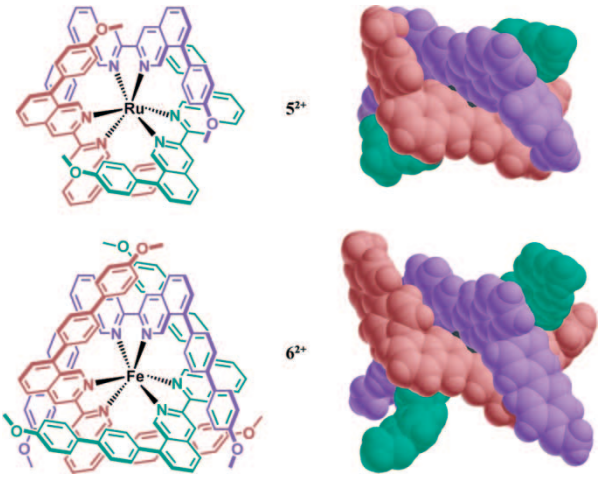

Figure 1. Left: Chemical structures of [Ru(8,8′-dianisyl-3,3′-biisoquinoline)$_3$]$^{2+}$ and [Fe(8,8′-diphenylanisyl-3,3′-biisoquinoline)$_3$]$^{2+}$. Right: X-ray crystal structures of these complexes (*26*).

through the application of an external stimulus. At least two stations are needed on the molecular axis between which the molecular ring may shuttle back and forth. The approach of the Sauvage group is based on the use of bi- and tri-dentate chelate ligands as stations on the axis, and macrocycles incorporating bidentate ligands as gliding rings, whereby the two components are held together by Cu(I/II) ions (*13*, *44–46*). The external stimulus triggering the molecular movement is of electrochemical nature: the change in metal oxidation state induces the shuttling motion. The working principle of such a two-station molecular shuttle is illustrated in Scheme 3.

At the starting point (top left), copper is in its + I oxidation state for which tetrahedral coordination is thermodynamically preferred, hence; the Cu(I) ion is co-ordinated to the two bidentate ligands. Cu(II), by contrast, prefers higher coordination numbers. Therefore, immediately after oxidation (top right), the copper ion finds itself in a thermodynamically unstable coordination environment. The consequence is de-coordination of the Cu(II) ion from the bidentate chelate on the molecular axis and translation of the Cu(II)-macrocycle moiety to the station offering the terdentate ligand (bottom right). Upon reduction of Cu(II), an unstable five-coordinate Cu(I) complex will be formed temporarily (bottom left), and this induces the back-shuttling of the metal-macrocycle entity to the starting point.

These molecular shuttles are usually true rotaxanes, i.e. there are bulky groups attached to the two ends of the molecular axis, preventing the macrocycle from de-threading. Hence, the shuttling process is usually highly reversible.

Scheme 4 shows a specific example of such a molecular two-station shuttle that was prepared and studied by the Strasbourg group (*13*). In this compound, the molecular axis is flexible, which makes it difficult to have a clear view of the geometry and the exact distance between the two stations of the shuttle. Moreover, in the thermodynamically stable tetrahedral Cu(I) complex, the metal centre is almost completely isolated from the chemical environment: the two sterically demanding dpp ligands shield the copper from the solvent. Thus, upon oxidation to Cu(II), the

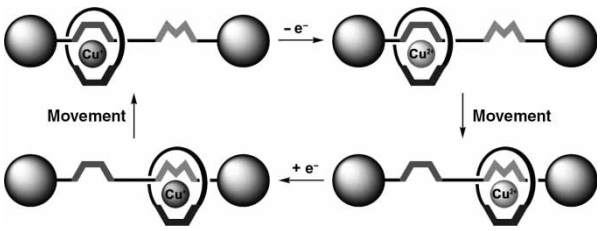

Scheme 3. Working principle of a two-station molecular shuttle comprised of a molecular axis with a bidentate chelate (e.g. a dpp-fragment) and a tridentate ligand (e.g. a terpyridine chelate). The molecular ring is typically a macrocycle incorporating a dpp-fragment.

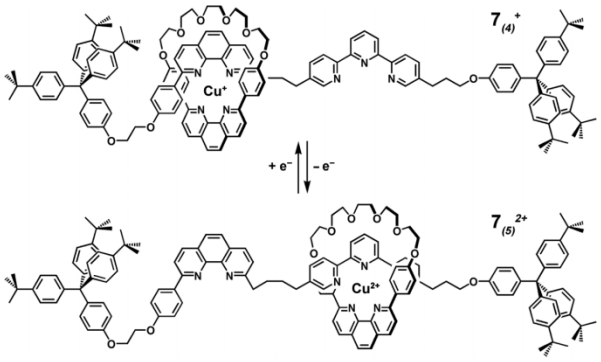

Scheme 4. Two-station molecular shuttle with a relatively flexible molecular axis containing a dpp station and a terpyridine station and a 30-membered macrocycle incorporating a dpp chelate.

resulting thermodynamically unstable $[Cu(dpp)_2]^{2+}$ complex stays kinetically inert, because the transient formation of a mobile solvent complex of Cu(II) is made difficult. As a consequence, the rearrangement of the thermodynamically unstable four-coordinate species $Cu_{(4)}$(II) to the five-coordinate species $Cu_{(5)}$(II), i.e. the gliding motion of the copper centre plus macrocycle along the molecular axis, takes place only on a minute to hour timescale (*13*). The same is true for the reverse process: when Cu(II) is reduced while being coordinated to the terpyridine station and the macrocyclic dpp-ligand, the resulting five-coordinate species $Cu_{(5)}$(I) is also kinetically inert, and the thermodynamically preferred four-coordinate species $Cu_{(4)}$(I) is formed equally slowly. In other words, both the forward and backward shuttling kinetics are very slow.

As shown recently for 'pirouetting' copper-complexed rotaxanes, decreasing the steric congestion around the copper coordination centre has a strong effect on the rearrangement rates of the complexes (*47*). Therefore, we reasoned that by using a macrocycle that incorporates the sterically non-hindering dpbiiq fragment **3** instead of the dpp-fragment **1**, the shuttling kinetics of our molecular

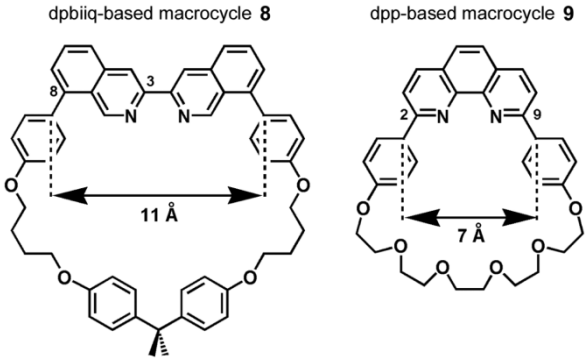

Scheme 5. A 39-membered macrocycle with the dpbiiq ligand motif and a 30-membered macrocycle with the dpp fragment.

machines might be improved. Towards this end, we have prepared macrocycle **8** (Scheme 5), which is considerably bigger than the dpp-based macrocycle **9**, which was used in the molecular shuttle from Scheme 4. The new macrocycle **8** is 39-membered and provides an inner cavity that is about 11 Å wide, whereas the dpp-based macrocycle **9** is only 30-membered with an inner cavity of roughly 7 Å width.

We have used the sterically less congesting macrocycle **8** as the mobile part in a new molecular shuttle (Scheme 6). In this rotaxane, the molecular axis differs from the previously used axis (Scheme 4) in several respects. The most important difference is that the phenanthroline and the terpyridine stations are now connected via a rigid *p*-phenylene spacer. This makes the new axis significantly less flexible than that of the rotaxane from Scheme 4.

The electrochemically triggered translation of the copper-complexed ring between the dpp and the terpy stations of the molecular axis was investigated using cyclic voltammetry, by analogy with previously described copper-containing bistable catenanes and rotaxanes (*10*, *11*, *13*). Through variation of the potential scan rate, it is possible to obtain kinetic information on the gliding motion of the macrocycle (*48*, *49*). A few representative cyclic voltammograms (CVs) are shown in Figure 2.

At the starting point of our CV experiments, molecular shuttle **10** from Scheme 6 has Cu(I) coordinated to dpp on the axis and dpbiiq on the macrocycle. At all scan rates, we observe only one single wave in the oxidative scan, centred around 0.48 V vs. saturated calomel electrode (SCE). This wave corresponds to oxidation of four-coordinate Cu(I). In the reductive sweep at low scan rates (50 mV/s), we observe a wave that is centred around 0.07 V vs. SCE which is due to the reduction of Cu(II) in a five-coordinate environment. This indicates that by the time the reductive sweep begins, the shuttling motion from the bidentate dpp station to the terdentate terpy-station has already taken place. When the scan rate is increased to 400 mV/s, a second reductive wave becomes observable. This wave is centred around 0.42 V vs. SCE and is attributed to the reduction of Cu(II) in a four-coordinate environment. This is a clear indication that under these experimental conditions, some of the molecular shuttles did not have sufficient time to undergo the gliding motion that should have followed Cu(I) to Cu(II) conversion in the oxidative sweep. Interestingly, an oxidation wave that could be associated with Cu(I) oxidation in a five-coordinate environment cannot be observed even at a scan rate of 1000 mV/s. This indicates that the gliding motion from the terpy to the dpp station following Cu(II) reduction is significantly faster than the reverse gliding motion that follows Cu(I) oxidation. This finding is in line with the previous observations on other molecular machines investigated by the Strasbourg group (*10*, *13*, *50–53*).

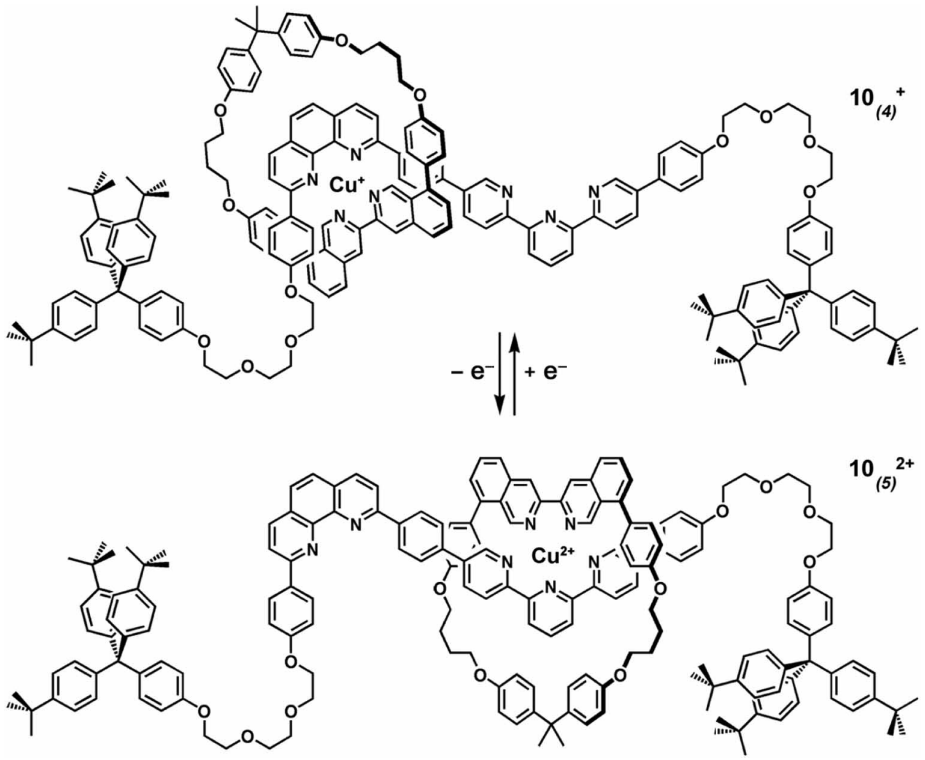

Scheme 6. A copper-based molecular shuttle with a rigid axis and a sterically non-hindering macrocycle.

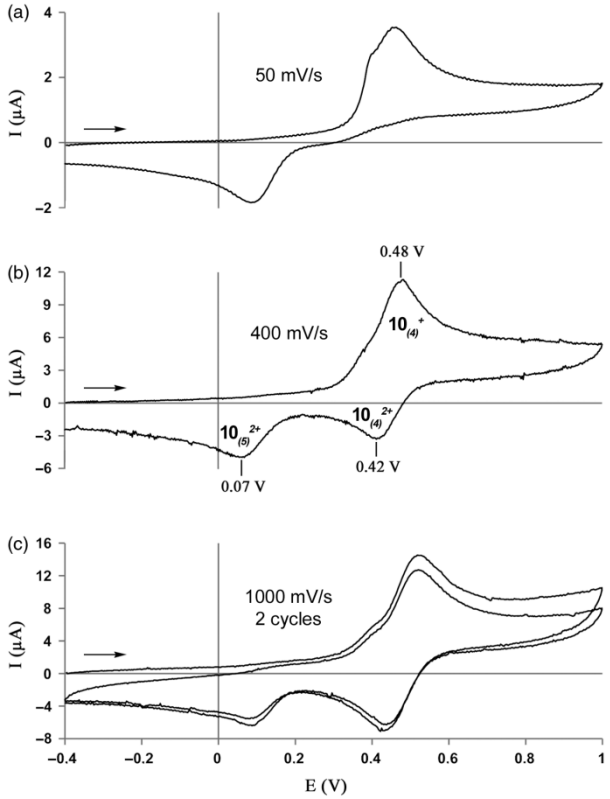

Figure 2. CVs obtained on the molecular shuttle from Scheme 6 at three different potential scan rates. See Ref. (*45*) for experimental details. Potentials are reported vs. SCE.

From these cyclic voltammetry experiments, we extract the following rate constants for the back-and-forth motion of macrocycle **8** in molecular shuttle **10**:

$$\mathbf{10}_{(4)}^{+} - e^{-} \rightarrow \mathbf{10}_{(4)}^{2+} \quad \text{Cu(I) oxidation}$$

$$\mathbf{10}_{(4)}^{2+} \rightarrow \mathbf{10}_{(5)}^{2+} \quad \text{gliding,} \quad k = 2\,s^{-1}$$

$$\mathbf{10}_{(5)}^{2+} + e^{-} \rightarrow \mathbf{10}_{(5)}^{+} \quad \text{Cu(II) oxidation}$$

$$\mathbf{10}_{(5)}^{+} \rightarrow \mathbf{10}_{(4)}^{+} \quad \text{gliding,} \quad k > 50\,s^{-1}.$$

For comparison, in molecular shuttle **7**, the rate constants for the two gliding motions are at least two orders of magnitude lower. It is tempting to attribute this dramatic acceleration fully to the sterically non-hindering nature of the new dpbiiq-based macrocycle, yet it must be noted that shuttles **7** and **10** differ also in the nature of the molecular axis. In shuttle **7**, there is a flexible axis with an alkane linker between the two stations, whereas in shuttle **10** there is a rigid axis with a *p*-phenylene spacer. In order to eliminate any doubts regarding the origin of the improved shuttling kinetics, we have investigated molecular shuttle **11** that is comprised of the same rigid axis as shuttle **10**, but with the sterically congesting 30-membered dpp-based macrocycle **9** (Scheme 7).

The difference in gliding kinetics between shuttles **10** and **11** is remarkable. As discussed above, in the shuttle with the biisoquinoline-macrocycle, gliding from the phenanthroline station to the terpyridine station following Cu(I) oxidation occurs within less than a second. By contrast, after Cu(I) oxidation of rotaxane **11**, the thermodynamically unstable four-coordinate species is stable for several hours. Thus, it is obvious that there exists a pronounced kinetic biisoquinoline effect.

The endocyclic but sterically non-protecting non-hindering nature of dpbiiq is the key to this spectacular improvement. Besides this non-hindering character, another important structural difference between dpp and the biisoquinoline ligand is the less rigid nature of the latter. Whereas dpp contains a rigid backbone, the biisoquinoline is able to rotate around its C_3—$C_{3'}$ bond, and this may facilitate de-coordination from a metal centre through stepwise de-complexation of one nitrogen donor atom after the other.

With these encouraging results at hand, it became realistic to envision molecular shuttles in which the translational motion occurs over a significantly longer distance (*54*, *55*) than in the prior systems. This vision included the use of a molecular axis with three instead of only two stations: the end stations should be comprised of the bidentate 1,10-phenanthroline ligand (dpp) to the host preferably Cu(I) and the terdentate terpyridine chelate to the host preferably Cu(II) as in the shuttles from Schemes 6

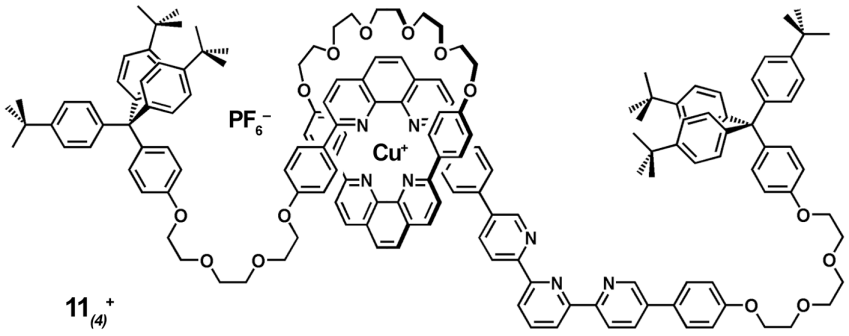

Scheme 7. A molecular shuttle comprised of the same rigid axis as the shuttle from Scheme 6, but with the smaller macrocycle **9** instead of the sterically non-hindering macrocycle **8**.

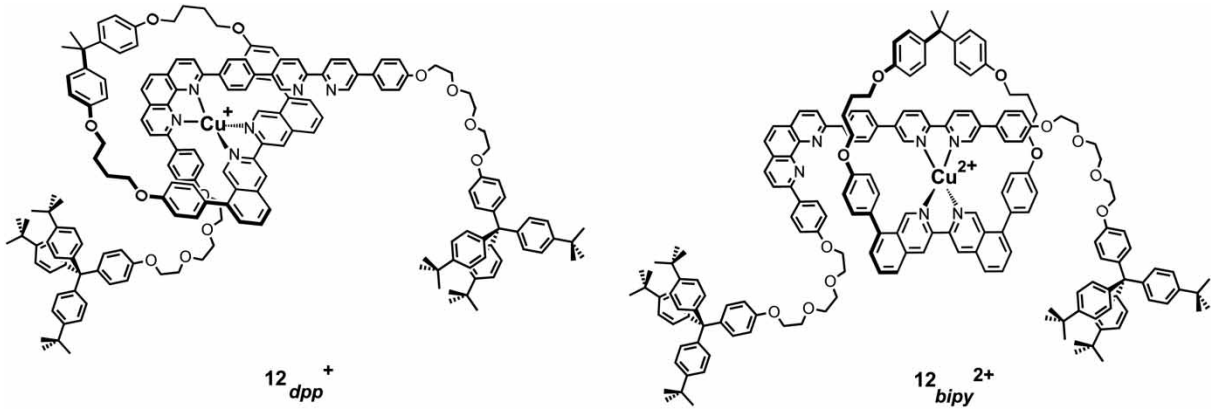

Scheme 8. A phenanthroline–bipyridine two-station shuttle in its two different forms $\mathbf{12}^{+}_{dpp}$ and $\mathbf{12}^{2+}_{bipy}$; the subscripts *dpp* and *bipy* indicate the position of the mobile ring (macrocycle **8**) on the molecular axis.

and 7. The hypothesis was that a 2,2′-bipyridine ligand could serve as an intermediate station that can facilitate the shuttling motion between the two end points. With this ultimate goal in mind, it seemed reasonable to explore in the first step the coordination chemistry and electrochemical behaviour of a two-station shuttle containing only a 1,10-phenanthroline (dpp) and a bipyridine (bipy) station. The resulting system, rotaxane **12** (*56*), is shown in Scheme 8.

By contrast to the molecular shuttles previously investigated by the Strasbourg group (*13*, *44–46*), this shuttle contains exclusively bidentate ligands and no terdentate chelates at all. Thus, even Cu(II) will only achieve a fourfold coordination as far as the nitrogen atoms of the chelates are concerned. However, it should be kept in mind that when the coordination sphere around these chelates is sterically not too demanding, there may be solvent molecules or anions that can coordinate to Cu(II), thereby satisfying its demand for higher coordination numbers. Indeed, the steric properties of the phenanthroline and bipyridine stations are vastly different: the former is highly shielding and prevents the copper centre from interacting with the chemical environment, and uptake of solvent molecules or anions as additional ligands is very difficult in this coordination site. The bipyridine station, on the other hand, is sterically much less demanding. Thus, it can be expected that additional ligation of solvent molecules or counterions will stabilise Cu(II) when coordinated to the bipyridine station, thereby making this the thermodynamically preferred station for the metal in its divalent oxidation state.

The relative thermodynamic stabilities between the Cu(I) and Cu(II) complexes formed in the molecular shuttle define the driving force for the shuttling motion. Evidently, the thermodynamic stability of Cu(II) in a bipyridine–biisoquinoline coordination environment (as the case for shuttle **12** of Scheme 8) will differ from the thermodynamic stability of Cu(II) in a terpyridine–biisoquinoline coordination (as the case for shuttle **10** of Scheme 6). As a consequence, the driving force for the ring translation in the phenanthroline–bipyridine shuttle will be different from that in the phenanthroline–terpyridine shuttle. This driving force can be estimated from the redox potentials of the various copper complexes. For shuttle **10**, the relevant data can be extracted from the CVs in Figure 2: the $[Cu(dpbiiq)(dpp)]^{+}$ complex is oxidised at 0.46 V vs. SCE, the $[Cu(dpbiiq)(terpy)]^{2+}$ species is reduced at 0.07 V vs. SCE. Hence, the driving force ΔG for ring translation in the phenanthroline–terpyridine shuttle is roughly 0.39 eV. In order to estimate the driving force for the phenanthroline–bipyridine shuttle, the model complexes shown in Scheme 9 were synthesised and investigated electrochemically.

From the redox potentials of the $[Cu(dpbiiq)(dpp)]^{+}$ and $[Cu(dpbiiq)(bipy)]^{2+}$ complexes, one estimates a driving force of only 0.16 eV for the phenanthroline-to-bipyridine gliding motion. Thus, the driving forces for the shuttling process differ significantly between rotaxane **10** and rotaxane **12**. The relatively low oxidation potential of the $[Cu(dpbiiq)(bipy)]^{+}$ complex (0.18 V vs. SCE) is indicative of a stabilisation of the Cu(II) oxidation state that is likely to be caused by a rearrangement of the coordination sphere to square planar or even octahedral geometry.

With this basic knowledge at hand, we undertook an electrochemical study of the new phenanthroline–bipyridine shuttle (*56*), similar to that discussed above for the phenanthroline–terpyridine system, using different potential scan rates to obtain kinetic information on the shuttling motion. Representative cyclic voltammetry data resulting from this work are shown in Figure 3.

Through comparison of the three data sets in Figure 3, the assignment of the different redox waves observed for shuttle **12** becomes straightforward: the oxidative wave of shuttle **12** around 0.42 V vs. SCE is also observed in the voltammogram of $[Cu(dpbiiq)(dpp)]^{+}$ reference complex **13** and therefore can be assigned to Cu(I) oxidation with

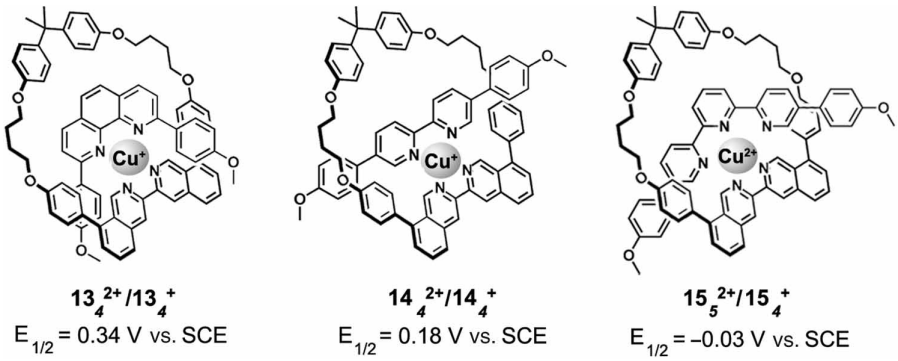

Scheme 9. Reference complexes for electrochemical investigations.

the macrocyle located at the 1,10-phenanthroline station. In the voltammogram of complex **13**, there is an additional oxidation wave around 0.65 V vs. SCE that we attribute to a $[Cu(dpp)_2]^+$ impurity that is formed under the experimental conditions used for the synthesis of **13**. This seems to be inevitable due to the high thermodynamic stability of the $[Cu(dpp)_2]^+$ complex. The reductive sweep of shuttle **12** exhibits a wave around 0.18 V, which coincides with the reduction wave observed in the voltammogram of $[Cu(dpbiiq)(bipy)]^{2+/+}$ reference complex **14** rather than with the reduction wave observed for $[Cu(dpbiiq)(dpp)]^{2+/+}$ reference complex **13**. This is a clear indication that at the potential scan rate used for the experiments in Figure 3 (100 mV/s), by the time the oxidative sweep is finished and the reductive sweep begins, the copper-macrocycle entity has already travelled from its initial position at the phenanthroline station to the bipyridine station. By analogy to our prior investigations, we varied the potential scan rates to obtain information on the shuttling kinetics. Figure 4 shows a series of voltammograms obtained during this work.

As the scan rate is increased from 200 to 800 mV/s and finally 1600 mV/s, there are no significant alterations in

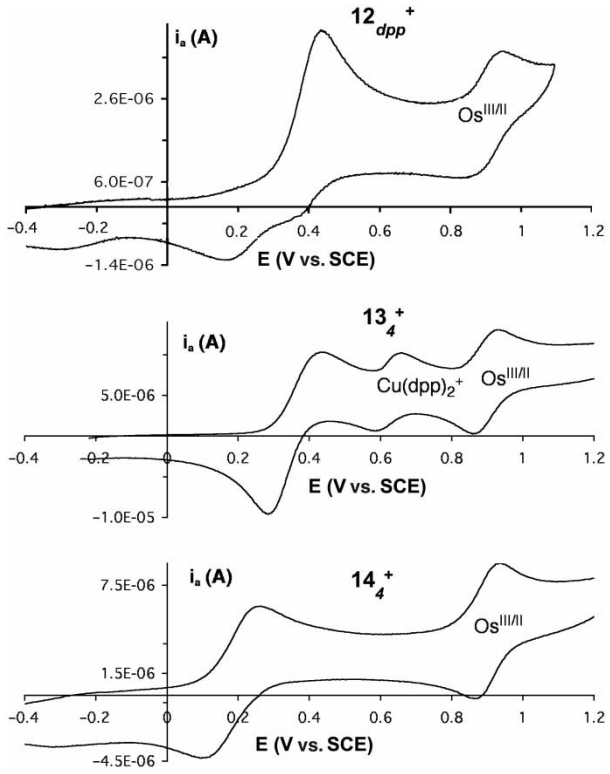

Figure 3. CVs of shuttle **12** and the reference complexes **13** and **14** recorded on a Pt working electrode in CH_2Cl_2—CH_3CN (1:9) with 0.1 M Bu_4NPF_6 at 100 mV/s. The reversible redox couple at 0.9 V vs. SCE is due to $Os(tterpy)_2^{2+}$ (tterpy = 4′-*p*-tolyl-2,2′,6′,2″-terpyridine) which was used as an internal reference in this work.

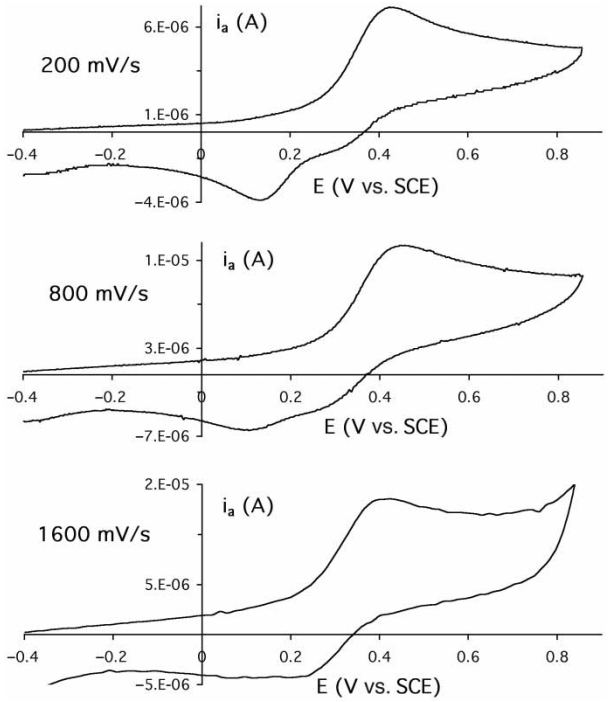

Figure 4. CVs of rotaxane **12** recorded at various potential scan rates in CH_2Cl_2—CH_3CN (1:9) with 0.1 M Bu_4NPF_6.

the oxidative sweep, but the reductive scan gradually changes. At 200 mV/s, one still observes the reduction wave associated with the $[Cu(dpbiiq)(bipy)]^{2+/+}$ complex, i.e. reduction of Cu(II) at the bipyridine station. At 1600 mV/s on the other hand, the reduction occurs at a significantly higher potential and coincides with the reduction wave observed for the $[Cu(dpbiiq)(dpp)]^{2+/+}$ complex **13** from Figure 3. This shows that at this scan rate, Cu(II) is reduced while located at the phenanthroline station. Under these experimental conditions, the travelling motion from the phenanthroline to the bipyridine station cannot keep up with the high potential scan rate: reduction of Cu(II) occurs while the metal is still in its initial coordination environment. Remarkable is the complete absence of an oxidative wave in the voltammogram of shuttle **12** that could be attributed to Cu(I) oxidation in a biisoquinoline–bipyridine coordination, even at the highest scan rate of 1600 mV/s. This indicates that the molecular movement originating from the unstable $[Cu(dpbiiq)(bipy)]^{+}$ complex is much faster than the shuttling motion originating from thermodynamically unstable $[Cu(dpbiiq)(dpp)]^{2+}$ complex. From our scan rate-dependent cyclic voltammetry experiments, a rate constant of $0.8\,s^{-1}$ can be extracted for the shuttling motion of macrocycle **8** from the dpp station to the bipy ligand, whereas for the reverse motion, a lower limit of $50\,s^{-1}$ is estimated. The magnitude of these rate constants is comparable to that for the dpp–terpy shuttle from Scheme 6, indicating that the lower thermodynamic driving force in the dpp–bipy shuttle from Scheme 8 is not a crucial factor as far as the shuttling kinetics are concerned.

With the dpp–terpy and dpp–bipy two-station shuttles completely characterised and identified as fully operational systems, the construction of a three-station shuttle comprised of one dpp, one bipy and a terpy station became a realistic goal. We have, therefore, prepared rotaxane **16** as shown in Scheme 10 (*29*).

The estimated distance between the two terminal coordination sites on the three-station molecular axis is 23 Å, which is considerably larger than in all previously investigated molecular shuttles of this type. Depicted in Scheme 10 are the thermodynamically stable forms for Cu(I) and Cu(II). From the studies of the two-station shuttles described above, the following order of thermodynamic stabilities for the individual copper complexes is expected: $[Cu(dpbiiq)(terpy)]^{+} < [Cu(dpbiiq)(bipy)]^{+} < [Cu(dpbiiq)(dpp)]^{+}$ for the Cu(I) species and a reversed order yielding $[Cu(dpbiiq)(dpp)]^{2+} < [Cu(dpbiiq)(bipy)]^{2+} < [Cu(dpbiiq)(terpy)]^{2+}$ for the Cu(II) species. Thus, the bipyridine ligand merely serves as an intermediate station to bridge the long distance between the two thermodynamically favoured positions. It was hoped that this, along with the fact that a sterically non-

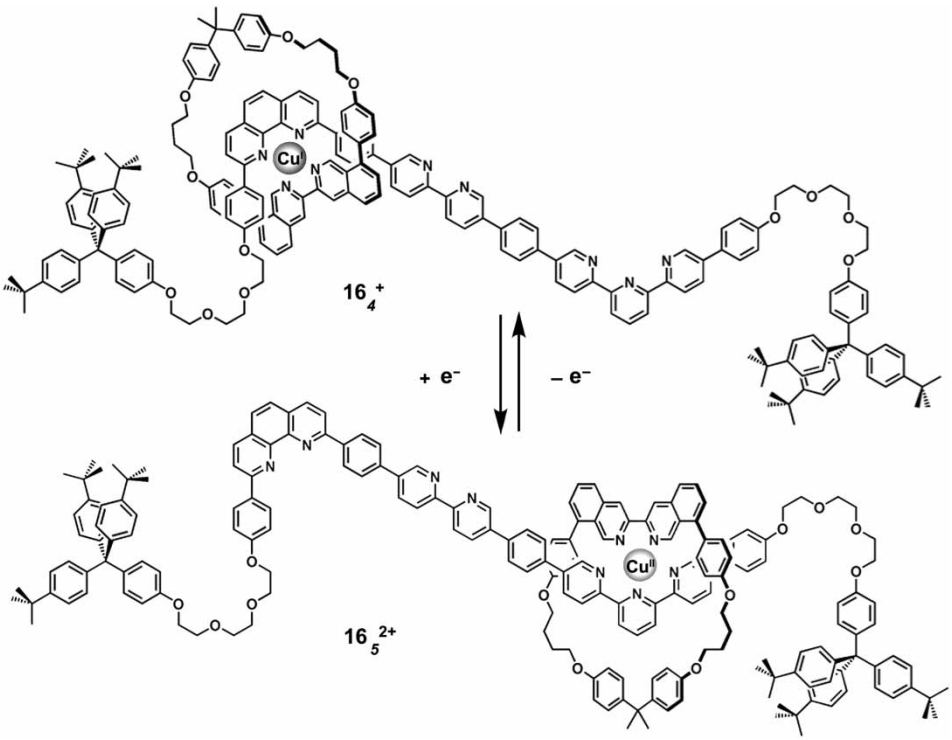

Scheme 10. Three-station rotaxane **16** containing dpp, bipy and terpy stations on the molecular axis and dpbiiq-based macrocycle **8**. The subscripts indicate the coordination numbers of the copper centre.

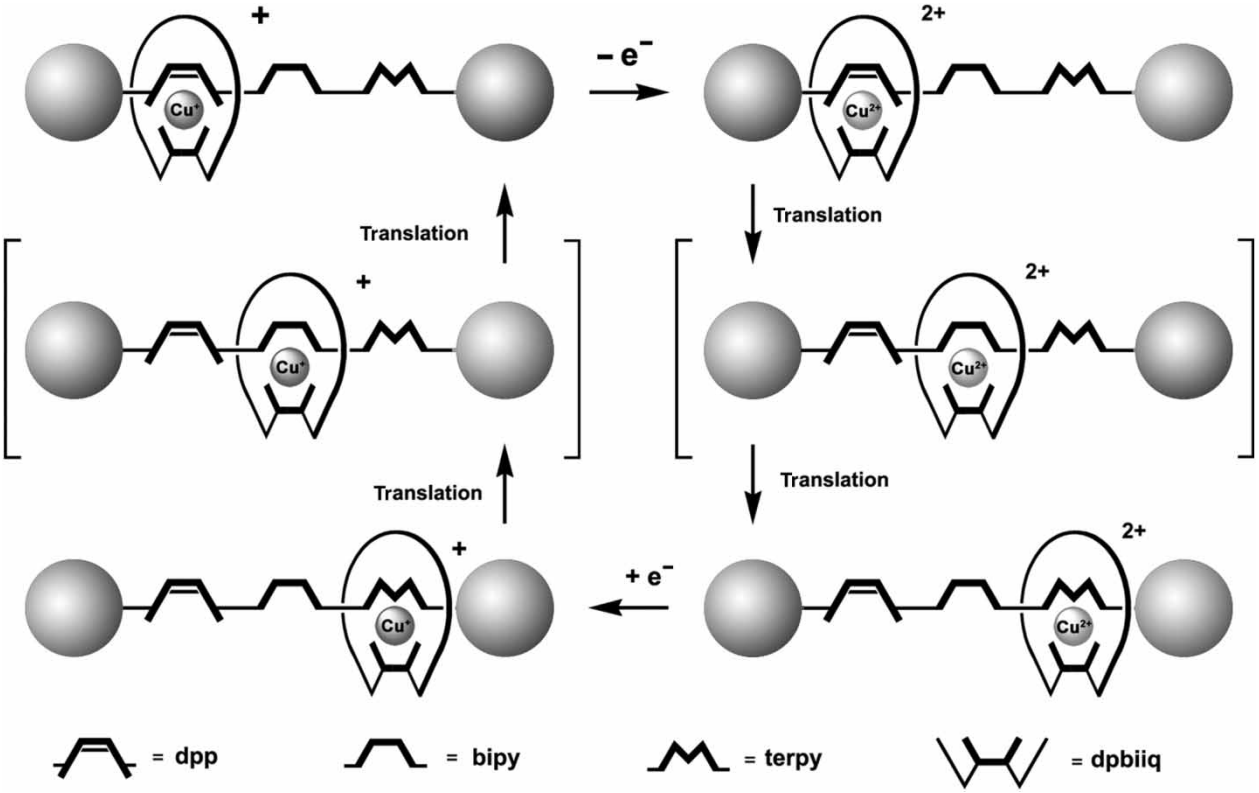

Scheme 11. Operating principle of the molecular three-station shuttle **16** from Scheme 10.

hindering dpbiiq-based macrocycle was threaded onto the molecular axis, would enable the molecular ring to move from one end to the other at reasonable rates. The expected shuttling sequence is illustrated in Scheme 11. Upon oxidation of Cu(I) to Cu(II), the metal centre and the ring are expected to travel from the initial dpp-position to the bipy station and from there onwards to the thermodynamically favoured terpy ligand (right half of Scheme 11). Upon reduction of the $[Cu(dpbiiq)(terpy)]^{2+}$ complex, the metal-macrocycle entity is anticipated to travel the reverse direction, again by way of the bipy station as a coordination site of intermediate stability (left half of Scheme 11).

CV was performed to investigate the shuttling processes in this long-distance shuttle. Figure 5 shows a comparison of the voltammograms obtained for three-station shuttle **16**, $[Cu(dpbiiq)(dpp)]^{+}$ reference complex **13**, $[Cu(dpbiiq)(bipy)]^{+}$ reference complex **14**, $[Cu(dpbiiq)(terpy)]^{2+}$ reference complex **15** and two-station dpp–terpy shuttle **10**.

From this comparison, assignment of the redox waves observed for the three-station shuttle **16** is straightforward: the oxidative wave observed for **16** at 0.38 V vs. SCE coincides with the wave at 0.37 V vs. SCE for two-station shuttle **10** and previously assigned to Cu(I) oxidation in four-coordinate dpbiiq–dpp environment. This assignment is in line with the oxidation potential of 0.38 V vs. SCE determined for $[Cu(dpbiiq)(dpp)]^{+}$ reference complex **13**. In the reductive sweep of the voltammogram of three-station shuttle **16**, there is only one clear reduction wave, and it is located at -0.02 V vs. SCE. This coincides with the reduction wave observed for $[Cu(dpbiiq)(terpy)]^{2+}$ reference complex **15**, and consequently can be assigned to reduction of Cu(II) in five-coordinate dpbiiq–terpy environment. The overall appearance of the voltammogram of three-station shuttle **16** is thus very similar to that of two-station dpp–terpy shuttle **10**: the same oxidation and reduction waves are observed, and there are no additional waves in the voltammogram of **16** that would be indicative of bipyridine-ligated copper. In other words, there is no electrochemical evidence for copper being coordinated to the intermediate bipy station. This observation suggests that translation away from the bipy ligand is fast in both directions: for Cu(II), bipy-to-terpy translation must be faster than dpp-to-bipy translation, and for Cu(I), bipy-to-dpp translation must be faster than terpy-to-bipy translation. Under these circumstances, the stationary concentration of the intermediate bipy-complex always stays low and its electrochemical signal cannot be detected. Indeed, from our experiments on the three-station shuttle, it is not clear whether the bipy ligand behaves as a real station that ligates to copper for a certain residence time.

Anyhow, scan-rate dependent cyclic voltammetry experiments similar to those presented in Figures 2 and

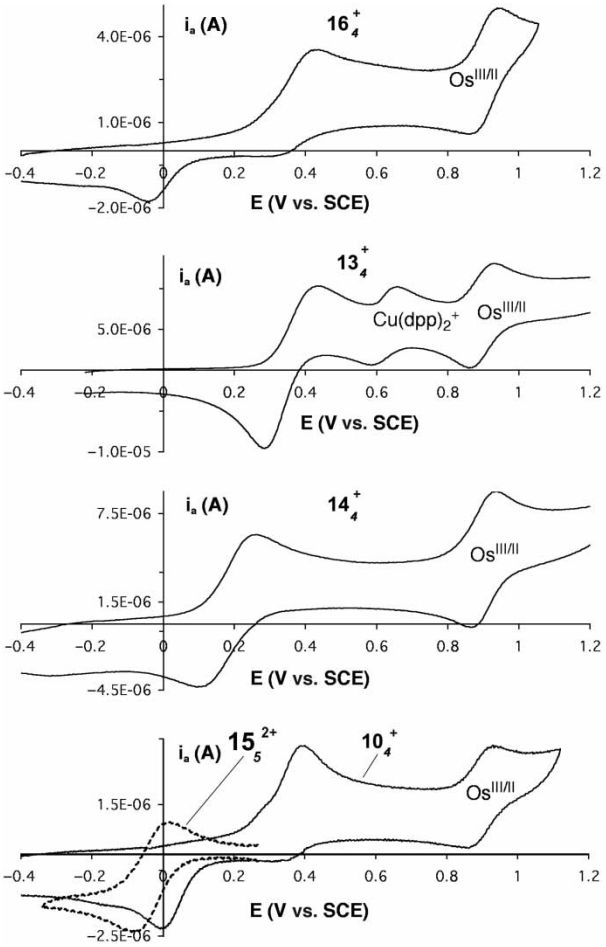

Figure 5. Comparison of the CVs for three-station shuttle **16**, $[Cu(dpbiiq)(dpp)]^+$ reference complex **13**, $[Cu(dpbiiq)(bipy)]^+$ reference complex **14**, $[Cu(dpbiiq)(terpy)]^{2+}$ reference complex **15** and two-station dpp–terpy shuttle **10**. The measurements were performed in CH_2Cl_2—CH_3CN (1:9) with 0.1 M Bu_4NPF_6 using a Pt working electrode and a scan rate of 100 mV/s. The reversible wave at 0.9 V vs. SCE is due to $Os(tterpy)_2^{2+}$ (tterpy = 4′-*p*-tolyl-2,2′,6′,2″-terpyridine) which was used as an internal reference.

4 allow us to estimate a rate constant of $0.4\,s^{-1}$ for the shuttling motion from the dpp site to the terpy ligand upon Cu(I) oxidation, and the reverse process following Cu(II) reduction occurs with $k \geq 50\,s^{-1}$.

3. Conclusions

The use of a sterically non-hindering biisoquinoline chelate allows the construction of molecular shuttles that exhibit greatly improved shuttling kinetics when compared to analogous systems that are based on sterically demanding macrocycles. When threaded on exactly the same molecular axis, a biisoquinoline-based 39-membered macrocycle moves several orders of magnitude more rapidly than a 30-membered phenanthroline-based macrocycle. When threaded onto a rigid molecular axis in which the overall distance between the two terminal stations is increased from roughly 11 Å to about 23 Å, the shuttling kinetics for the biisoquinoline-based macrocycle do not decrease significantly. While it is likely that the presence of a third station of intermediate thermodynamic stability facilitates shuttling over the 23 Å distance, there is no doubt that the key to these results is the biisoquinoline core of the mobile ring. With respect to the previously investigated phenanthroline-based systems, it may thus be stated that the new biisoquinoline-macrocycles are not only bigger, they also lead to faster shuttling kinetics in rotaxane-type molecular machines. Thus, bigger rings give rise to better performance due to faster molecular movements, and sterically non-hindering biisoquinoline chelates are truly bigger, better and faster.

Acknowledgements

We thank all the skilful and motivated researchers who contributed to this work, namely David Hanss, Alexander I. Prikhod'ko and Pirmin Roesel. Financial support from the Région Alsace (FD and JL), the European Commission and the Swiss National Science Foundation (OSW) is acknowledged. We thank Kari Rissanen and his group for X-ray crystallographic work.

References

(1) Amabilino, D.B.; Stoddart, J.F. *Chem. Rev.* **1995**, *95*, 2725–2828.
(2) Collier, C.P.; Wong, E.W.; Belohradsky, M.; Raymo, F.M.; Stoddart, J.F.; Kuekes, P.J.; Williams, R.S.; Heath, J.R. *Science* **1999**, *285*, 391–394.
(3) Harada, A. *Acc. Chem. Res.* **2001**, *34*, 456–464.
(4) Kinbara, K.; Aida, T. *Chem. Rev.* **2005**, *105*, 1377–1400.
(5) Kocer, A.; Walko, M.; Meijberg, W.; Feringa, B.L. *Science* **2005**, *309*, 755–758.
(6) Champin, B.; Mobian, P.; Sauvage, J.-P. *Chem. Soc. Rev.* **2007**, *36*, 358–366.
(7) Kay, E.R.; Leigh, D.A.; Zerbetto, F. *Angew. Chem., Int. Ed.* **2007**, *46*, 72–91.
(8) Green, J.E.; Choi, J.W.; Boukai, A.; Bunimovich, Y.; Johnston-Halperin, E.; Delonno, E.; Luo, Y.; Sheriff, B.A.; Xu, K.; Shin, Y.S.; Tseng, H.-R.; Stoddart, J.F.; Heath, J.R. *Nature* **2007**, *445*, 414–417.
(9) Balzani, V.; Venturi, M.; Credi, A. *Molecular Devices and Machines – Concepts and Perspectives for the Nanoworld*; Wiley: Weinheim, 2008.
(10) Livoreil, A.; Dietrich-Buchecker, C.O.; Sauvage, J.-P. *J. Am. Chem. Soc.* **1994**, *116*, 9399–9400.
(11) Cárdenas, D.J.; Livoreil, A.; Sauvage, J.-P. *J. Am. Chem. Soc.* **1996**, *118*, 11980–11981.
(12) Solladie, N.; Chambron, J.-C.; Dietrich-Buchecker, C.O.; Sauvage, J.-P. *Angew. Chem., Int. Ed.* **1996**, *35*, 906–909.
(13) Collin, J.-P.; Gaviña, P.; Sauvage, J.-P. *New J. Chem.* **1997**, *21*, 525–528.
(14) Colasson, B.; Dietrich-Buchecker, C.O.; Jimenez-Molero, M.C.; Sauvage, J.-P. *J. Phys. Org. Chem.* **2002**, *15*, 476–483.
(15) Frey, J.; Kraus, T.; Heitz, V.; Sauvage, J.-P. *Chem. Eur. J.* **2007**, *13*, 7584–7594.

(16) Schill, G. *Catenanes, Rotaxanes and Knots*; Academic Press: New York, 1971.
(17) Dietrich-Buchecker, C.O.; Sauvage, J.-P. *Chem. Rev.* **1987**, *87*, 795–810.
(18) Amabilino, D.B.; Stoddart, J.F. *Chem. Rev.* **1995**, *95*, 2725–2828.
(19) Sauvage, J.-P. *Acc. Chem. Res.* **1998**, *31*, 611–619.
(20) Sauvage, J.-P.; Dietrich-Buchecker, C.O. *Molecular Catenanes, Rotaxanes and Knots*; Wiley-VCH: Weinheim, 1999.
(21) Dietrich-Buchecker, C.O.; Sauvage, J.-P.; Kintzinger, J.-P. *Tetrahedron Lett.* **1983**, *24*, 5095–5098.
(22) Dietrich-Buchecker, C.O.; Sauvage, J.-P.; Kern, J.-M. *J. Am. Chem. Soc.* **1984**, *106*, 3043–3045.
(23) Durola, F.; Sauvage, J.-P.; Wenger, O.S. *Chem. Commun.* **2006**, 171–173.
(24) Durola, F.; Hanss, D.; Roesel, P.; Sauvage, J.-P.; Wenger, O.S. *Eur. J. Org. Chem.* **2007**, 125–135.
(25) Durola, F.; Wenger, O.S.; Sauvage, J.-P. *Helv. Chim. Acta* **2007**, *90*, 1439–1446.
(26) Durola, F.; Russo, L.; Sauvage, J.-P.; Rissanen, K.; Wenger, O.S. *Chem. Eur. J.* **2007**, *13*, 8749–8753.
(27) Ventura, B.; Barigelletti, F.; Durola, F.; Flamigni, L.; Sauvage, J.-P.; Wenger, O.S. *Dalton Trans.* **2008**, 491–498.
(28) Durola, F.; Sauvage, J.-P.; Wenger, O.S. *Coord. Chem. Rev.* **2010**, *254*, 1748–1759.
(29) Bissell, R.A.; Córdova, E.; Kaifer, A.E.; Stoddart, J.F. *Nature* **1994**, *369*, 133–137.
(30) Murakami, H.; Kawabuchi, A.; Kotoo, K.; Kunitake, M.; Nakashima, N. *J. Am. Chem. Soc.* **1997**, *119*, 7605–7606.
(31) Wurpel, G.W.H.; Brouwer, A.M.; van Stokkum, I.H.M.; Farran, A.; Leigh, D.A. *J. Am. Chem. Soc.* **2001**, *123*, 11327–11328.
(32) Stanier, C.A.; Alderman, S.J.; Claridge, T.D.W.; Anderson, H.L. *Angew. Chem., Int. Ed.* **2002**, *41*, 1769–1772.
(33) Chang, S.-Y.; Jeong, K.-S. *J. Org. Chem.* **2003**, *68*, 4014–4019.
(34) Keaveney, C.M.; Leigh, D. *Angew. Chem., Int. Ed.* **2004**, *43*, 1222–1224.
(35) Pérez, E.M.; Dryden, D.T.F.; Leigh, D.A.; Teobaldi, G.; Zerbetto, F. *J. Am. Chem. Soc.* **2004**, *126*, 12210–12211.
(36) Wang, Q.-C.; Qu, D.-H.; Ren, J.; Chen, K.; Tian, H. *Angew. Chem., Int. Ed.* **2004**, *43*, 2661–2665.
(37) Korybut-Daszkiewicz, B.; Wieckowska, A.; Bilewicz, R.; Domagała, S.; Wozniak, K. *Angew. Chem., Int. Ed.* **2004**, *43*, 1668–1672.
(38) Balzani, V.; Clemente-León, M.; Credi, A.; Ferrer, B.; Venturi, M.; Flood, A.H.; Stoddart, J.F. *Proc. Natl Acad. Sci.* **2006**, *103*, 1178–1183.
(39) Sindelar, V.; Silvi, S.; Kaifer, A.E. *Chem. Commun.* **2006**, 2185–2187.
(40) Hirose, K.; Shiba, Y.; Ishibashi, K.; Doi, Y.; Tobe, Y. *Chem. Eur. J.* **2008**, *14*, 3427–3433.
(41) Umehara, T.; Kawai, H.; Fujiwara, K.; Suzuki, T. *J. Am. Chem. Soc.* **2008**, *130*, 13981–13988.
(42) Fioravanti, G.; Haraszkiewicz, N.; Kay, E.R.; Mendoza, S.M.; Bruno, C.; Marcaccio, M.; Wiering, P.G.; Paolucci, F.; Rudolf, P.; Brouwer, A.M.; Leigh, D.A. *J. Am. Chem. Soc.* **2008**, *130*, 2593–2601.
(43) Coutrot, F.; Busseron, E. *Chem. Eur. J.* **2009**, *15*, 5186–5190.
(44) Durola, F.; Sauvage, J.-P. *Angew. Chem., Int. Ed.* **2007**, *46*, 3537–3540.
(45) Durola, F.; Lux, J.; Sauvage, J.-P. *Chem. Eur. J.* **2009**, *15*, 4124–4134.
(46) Collin, J.-P.; Durola, F.; Lux, J.; Sauvage, J.-P. *Angew. Chem., Int. Ed.* **2009**, *48*, 8532–8535.
(47) Collin, J.-P.; Durola, F.; Mobian, P.; Sauvage, J.-P. *Eur. J. Inorg. Chem.* **2007**, 2420–2425.
(48) Nicholson, R.S.; Shain, I. *Anal. Chem.* **1964**, *36*, 706–723.
(49) Raehm, L.; Kern, J.-M.; Sauvage, J.-P. *Chem. Eur. J.* **1999**, *5*, 3310–3317.
(50) Collin, J.-P.; Gaviña, P.; Sauvage, J.-P. *Chem. Commun.* **1996**, *17*, 2005–2006.
(51) Kern, J.-M.; Raehm, L.; Sauvage, J.-P.; Divisia-Blohorn, B.; Vidal, P.-L. *Inorg. Chem.* **2000**, *39*, 1555–1560.
(52) Poleschak, I.; Kern, J.-M.; Sauvage, J.-P. *Chem. Commun.* **2004**, 474–476.
(53) Létinois-Halbes, U.; Hanss, D.; Beierle, J.M.; Collin, J.-P.; Sauvage, J.-P. *Org. Lett.* **2005**, *7*, 5753–5796.
(54) Lane, A.S.; Leigh, D.A.; Murphy, A. *J. Am. Chem. Soc.* **1997**, *119*, 11092–11093.
(55) Tseng, H.-R.; Vignon, S.A.; Stoddart, J.F. *Angew. Chem., Int. Ed.* **2003**, *42*, 1491–1495.
(56) Collin, J.-P.; Durola, F.; Lux, J.; Sauvage, J.-P. *New J. Chem.* **2010**, *34*, 34–43.